STRESS-STRAIN FIELD AND THEORETICAL ANALYSIS OF RC BRIDGE

A.A. Maghsoudi* and F. Azadpour

Department of Civil Engineering, Shahid Bahonar University
P.O. Box 76169-133, Kerman, Iran
maghsoudi.a.a@mail.uk.ac.ir - fa_azadpour@yahoo.com

*Corresponding Author

(Received: December 24, 2006 – Accepted in Revised Form: September 25, 2008)

Abstract In this paper, a reinforced concrete(RC) bridge built in an interchange, in the city of Kerman (a city located in south of Iran) is examined by the Structural Health Monitoring (SHM) system. During the construction of this bridge such as; the main beams, slab, and retaining walls, some Electrical Strain Gauges were mounted on the main reinforcements at different locations within the body of this bridge. After the completion, the bridge was loaded with different load arrangements and the strain readings were collected by a powerful Data Logger for field analysis. The considered loading cases were, 1) twelve trucks carrying sand with an average weight of 28t each, the trucks were lined up in regular pattern and also in a certain preprogrammed arrangement, 2) the daily traffic loads, the bridge behavior was examined and data were recorded during the peak points of the daily traffic, 3) the bridge weight, to find this, the traffic was not allowed to pass over the bridge for a few days, in order to record the bridges' behavior under its own weight. All loadings and unloading cases were recorded for field analysis. The theoretical analysis of the bridge was performed according to the classical method. To achieve the best findings, also the Finite Element program- ANSYS -was used, for all loading cases. This program is able to model concrete reinforcement by its own library elements. Concrete could also be studied as a nonlinear element. Finally, the field analysis and theoretical findings were compared and the results are presented.

Keywords Field and Theoretical Analysis, Electrical Strain Gauges, RC Bridge, Monitoring, ANSYS

چکیده در مقاله حاضر، پل بتنی واقع در تقاطع میدانی در استان کرمان (استانی واقع در جنوب ایران) با روش رفتارنگاری صحت سازه ای Structural Health Monitoring, SHM بررسی شده است. در حین اجرای مراحل مختلف، اعضای این پل بتن مسلح از جمله تیرهای اصلی، عرشه و دیوارهای حائل، حس گرهای الکتریکی کرنش سنج بر میلگردهای اصلی در نقاط مختلف اعضای سازه ای نصب شد. پس از اتمام مراحل ساخت و در حین بهره‌برداری، پل مزبور با چیدمان های مختلف، بارگذاری گردید. کرنش ایجاد شده در میلگردها، ناشی از بارگذاری، به‌کمک دستگاه ثبت داده ها Data Logger برای تحلیل میدانی پل برداشت شد. حالت‌های مختلف بارگذاری عبارتند از (۱) دوازده عدد کامیون با وزن متوسط ۲۸ تن مصالح برای هر کامیون که با نظم مشخصی پشت‌سرهم قرارگرفتند، (۲) بارهای ترافیک روزمره به عبارت دیگر رفتار پل تحت بار ترافیک حداکثر روزانه در این حالت مورد نظر بوده است و (۳) وزن پل که چند روز اجازه تردد وسائل نقلیه از روی آن داده نشد تا امکان برداشت داده‌های ناشی از عملکرد پل تحت وزن خود میسر گردد. برای هر حالت بارگذاری، کرنش ایجاد شده برداشت شد و تحلیل میدانی صورت گرفت. تحلیل تئوری پل نیز با روش کلاسیک انجام شد. همچنین به‌منظور رسیدن به بهترین دست‌آورد، از برنامه المان محدود انسیس ANSYS برای آرایش بارهای میدانی فوق نیز بهره‌گرفته شد. این برنامه قادر به مدل کردن بتن و میلگردها با توجه به المان های موجود می‌باشد. بتن را می‌توان همانند یک المان غیرخطی با عملکردی مشابه عملکرد واقعی خود در نظر گرفت. نتایج تحلیل میدانی و تحلیل تئوریک نهایتا مورد مقایسه قرار گرفته و نتایج بدست آمده از این مقایسه نیز ارائه گردید.

1. INTRODUCTION

All man-made structures have finite life spans and begin to degrade as soon as they are put into service. Processes such as corrosion, fatigue… degrade them until they are no longer fit for their

intended use. Depending on the value of the structure, a number of actions can be taken for the repair cost and the consequences of it are failing:

- Wait until it totally breaks and throw it away (low sticker price relative to repair cost, low criticality).
- Wait until it breaks and repair it (high sticker price relative to repair cost, low criticality).
- Examine it at certain intervals and decide whether or not remedial action is needed (high criticality). This is Structural Health Monitoring, SHM.

Many engineered structures such as bridges and buildings would fall in latter category. The consequences of a bridge collapsing are as such; that even though regular and necessary inspections are performed by skilled engineers to assess the health of the structures, nevertheless it is costly and usually finds no faults. It is also subject to human error, meaning that some unnecessary maintenance is performed and some faults go undetected. A SHM system consists of sensing and processing elements. A network of sensors measures relevant parameters, such as loads on structures (Figure 1). Signal processing and analysis routines relate the sensors' data about the structures' health to the owners and maintainers [1-3].

As an example, the use of on-site measurements to refine and improve an initial finite element model of a structure for subsequent detailed analytical investigations is invaluable. RAMBOLL, of Denmark, successfully used strain gauge measurements on the Forsmo Bridge in Sweden to fine-tune a LUSAS Bridge model prior to carrying-out an in-depth assessment of the structure for a proposed increase in freight train axle loading [4].

In this paper, a RC bridge is studied as RAMBOLL did. The concrete bridge located in an Interchange in the city of Kerman is examined by the SHM system. During the construction of the different elements of this reinforced concrete bridge, such as main beams, slab, and retaining walls, the Electrical Strain Gauges were mounted on the main reinforcements at different locations of the elements. For three different cases of loading, the strain readings were recorded by a powerful Data Logger for the field analysis. The literature study indicated that no SHM research report is presented for available bridges in this country.

The theoretical analysis of the bridge was performed by the classical method [5,6]. Different researchers are reported on modeling of different types of reinforced or prestressed concrete structures by the use of ANSYS modeling [7-10]. Here, also to achieve the best findings, the Finite Element program- ANSYS [10] was used, for all loading cases adopted in the field analysis. This program is capable of modeling reinforced concrete by its own library elements. Concrete could be studied in real as a nonlinear element. Finally, the field and theoretical analysis is compared and results are presented.

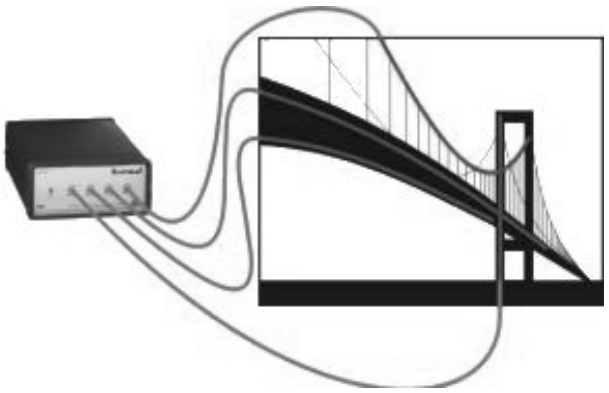

Figure 1. SHM for a steel bridge.

2. A BRIEF INTRODUCTION OF RC BRIDGE IN PAJOUHESH SQUARE

The Pajouhesh square is located just in front of Kerman University and it intersects three high ways from three different directions with heavy traffic flow. The plan and final views of the RC bridge is shown in Figure 2. As can be seen, the location of Kerman University is within the junction and the danger of its heavy traffic threatened the lives of the students, so the municipality of Kerman city, constructed the Pajouhesh square at the junction to reduce the disturbing serious factor. During the bridge construction and before casting the concrete,

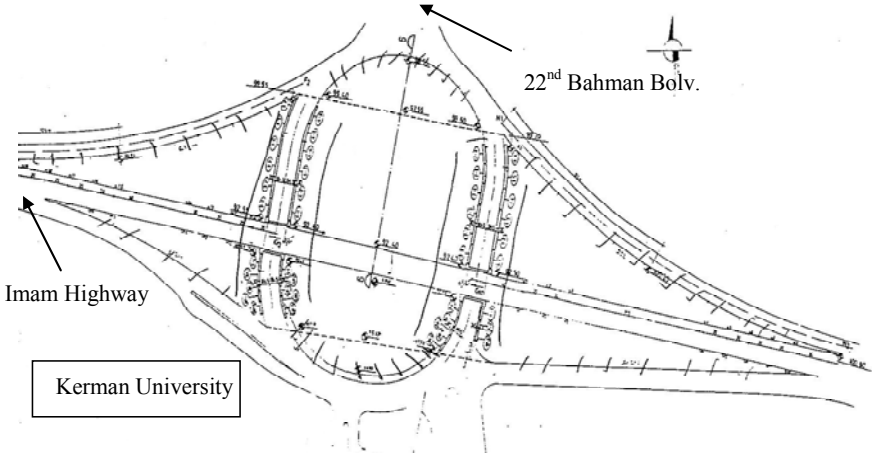

(a)

(b)

Figure 2. (a) The plan view of the RC bridge of pajouhesh and (b) View of the bridge in service.

25 Electrical Strain Gauges were mounted (by the first author) on the main reinforcements of the structural elements (Figure 6). Unfortunately, although cares were taken during handling and concrete casting of the structural elements, after the completion of the construction, it was found that some of the gauges were not active. Hence, the field analysis of the bridge is based on the remaining working Electrical Strain Gauges.

To install the Electrical Strain Gauge on the steel rebar, the rebar was torn at the position of gauge installation, degraded and then was polished to install the electrical strain gauges as well as possible (Figure 3).

The electrical strain gauges were waterproofed by a special coating to assure that the water in concrete has no effect on it. Finally, the strain gauges were covered by a special strip to prevent any damages due to concrete casting (Figure 4).

To assure that concrete pouring doesn't damage the strain gauges, the wires were passed though a hose i.e., a small diameter plastic tube (Figure 5).

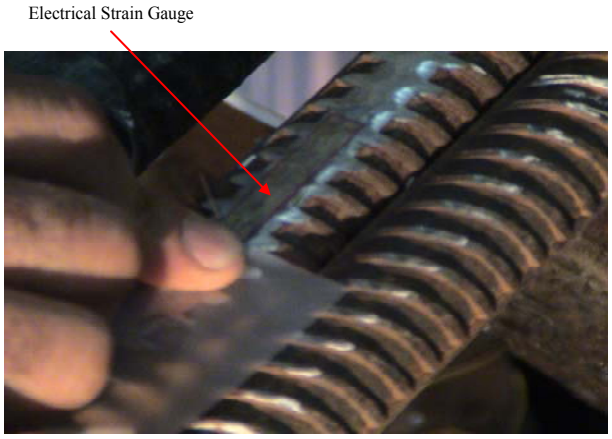

Figure 3. Fixing the electrical strain gauge on the steel bar.

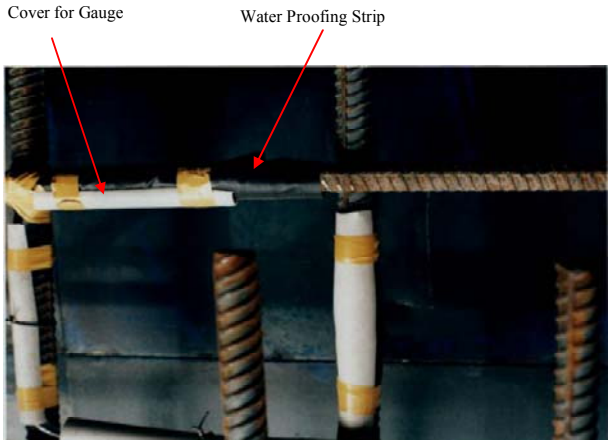

Figure 4. Covering of electrical strain gauges.

Figure 5. Passing the wire into the hose in RC wall.

3. ELECTRICAL STRAIN GAUGE DETAILS

For different diameter bar used as the structural elements of RC bridge, the following electrical strain gauges, which were made by TML Company of Japan were mounted on the rebar prior to concrete casting [5];

- Electrical strain gauge type: PFL-30-11, Gauge length 30mm, Gauge resistance 120 ± 0.3 Ω and Gauge factor 2.12 ± 1 %.
- Electrical strain gauge type: PFL-10-11, Gauge length 10mm, Gauge resistance 120± 0.3 Ω and Gauge factor 2.13 ± 1 %.
- Electrical strain gauge type: PFL-5-11, Gauge length 5mm, Gauge resistance 120 ± 0.3 Ω and Gauge factor 2.13 ± 1 %.
- Where Ω is in Ohm.

3.1. Field Analyzing of RC Bridge Under Traffic Load

For analyzing purpose, it was assumed that the X axis is on the structure joint, the Y axis is on the external reinforcement mesh and Z axis is in the vertical direction with the origin on the foundation. The coordinates and the position of strain gauges, S.G. is shown in Table 1 and Figure 6 respectively.

The bridge was analyzed for three applied traffic load arrangement. First, certain traffic load was defined as 12 trucks containing sand with an average weight of 28 ton each. The trucks were loaded on the bridge with a certain line pattern, as shown in Figure 7.

Immediately after settling the first loaded truck, (at 21:32 PM) the process of data recording began by Data Logger and continued at every 2 minutes intervals. According to the planned program, after settling the last truck on the bridge, the strain gauge data were recorded for few minutes (until 22:16 PM), then the trucks arrangement was changed and they were set in 3 parallel lines (Figure 8), and data was recorded.

The trucks were directed off the bridge in two parallel traffic lines (at 22:59:05 PM). The trucks were re-directed and loaded on the bridge again. This procedure was repeated several times. Finally, the data were recorded in the minimum possible time period. The diagrams of field strain versus the time of data readings are shown in Figures 9a to 9c.

TABLE 1. The Assumed Strain Gauges Coordinate Fixed on the Retaining Wall.

Coordinate	X(cm)	Y(cm)	Z(cm)	
			Horizontal Bar	Vertical Bar
S.G. 1	0.0	110	20	30
S.G. 2	0.0	550	20	30
S.G. 3	230	140	40	30
S.G. 6	0.0	365	20	30
S.G. 11	40	110	40	30
S.G. 12	40	365	20	30
S.G. 13	40	550	20	30
S.G. 14	230	100	----------	50
S.G. 15	230	560	----------	30
S.G. 16	0.0	110	740	----------
S.G. 18	0.0	550	740	----------
S.G. 20	40	110	----------	740
S.G. 21	0.0	110	----------	740
S.G. 24	40	550	----------	740
S.G. 25	0.0	550	----------	740

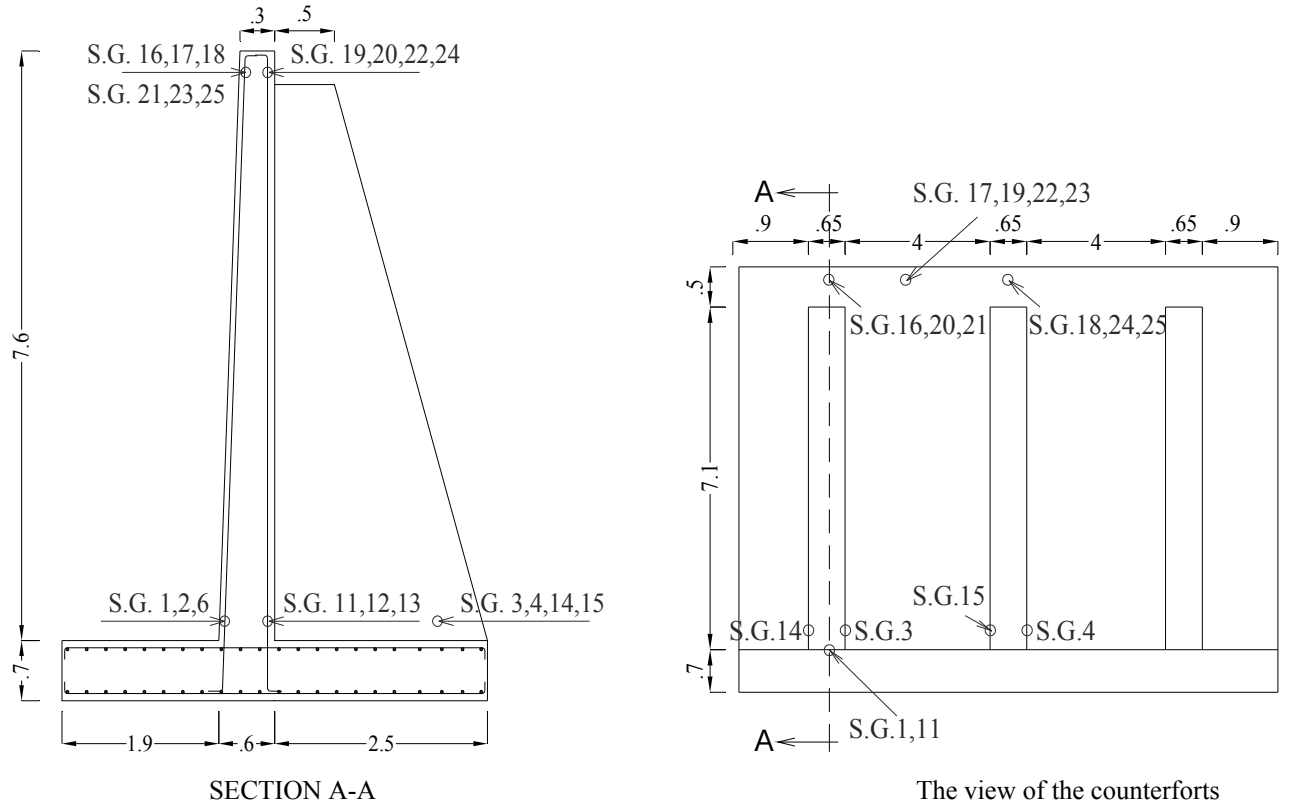

Figure 6. Position of strain gauges on RC wall.

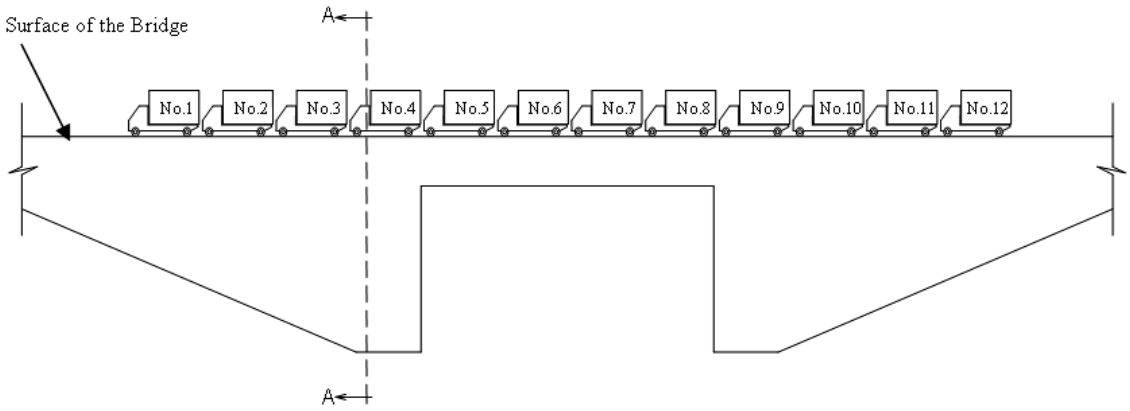

Figure 7. The trucks position on the bridge (stage 1).

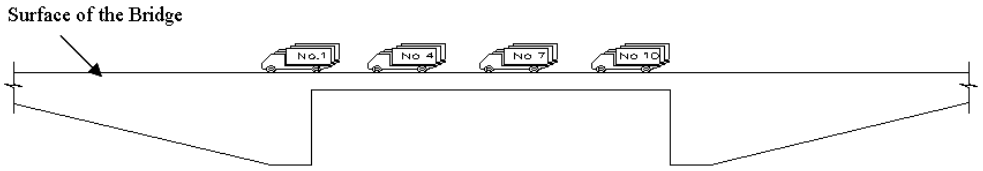

Figure 8. Location of the trucks on the bridge (stage 2).

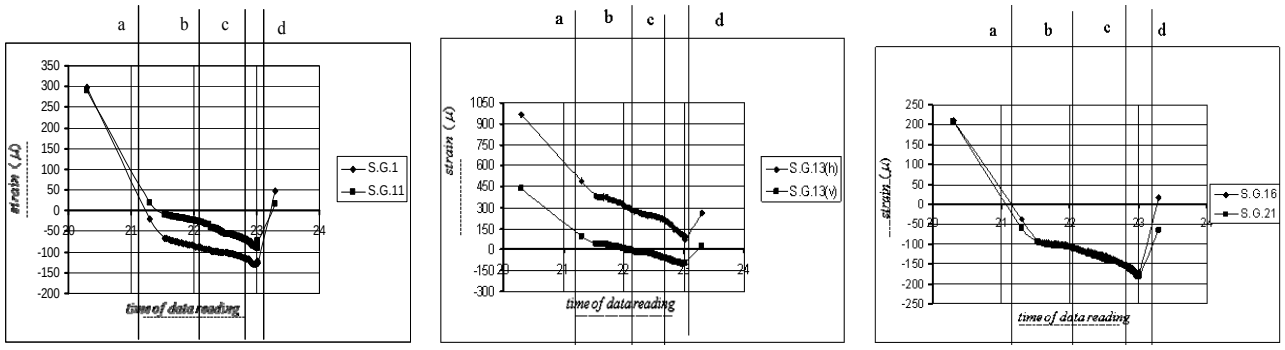

(a) (b) (c)

Figure 9. (a) Field strain values for gauge No. 1 and No. 11 for whole period of time considered due to loading, (b) field strain (horizontal and vertical) values for gauge No. 13 for whole period of time considered due to loading and (c) field strain values for gauge No. 16 and No. 21 for whole period of time considered due to loading, where, a-start of truck moving, b-trucks in 3 parallel lines, c-change the trucks arrangement in 2 lines, d-end of the trucks moving.

The curves show a clear demonstration of field behavior of the bridge during the loading and unloading periods. The main point after loading showed that, the curves returned back to its original position immediately. It is very clear that the curves have some plastic deformation, which could not reach the exact original positions.

3.2. Analyzing the Bridge under Traffic Load For the next case of loading, the daily traffic loads were considered at a weekend. Here, the strain readings were recorded continuously 24 hours a day. For more accuracy also the number of automobiles in the peak times of traffic (morning and afternoon) was recorded.

The automobiles were classified in two groups: (a) cars, (b) trucks and pickups. The groups with their number of passes are shown in Table 2 and 3. According to the data, the diagram is shown in Figure 10.

Based on the data taken by the Data Logger, the field strains versus time are shown in Figures 11 to 16. During the beginning hours of the day, when the flow of traffic was low, the curve shows a decrease. Whereas, from 8:0 A.M, when the traffic flow is heavier, the slope of the curves reverses and increases to its peak points at 4:0-5:0 P.M. The bridge is located in front of the university entrance so that, the traffic passing through depends on the activity of the student, classes and the official daily working hours, therefore as shown in Figures 11 to 16, after 5:0 P.M, the traffic flow as well as the slope of the curves decreased. Referring to Tables 2:0-3:0, during the period of 8:0-12:0 A.M, the number of automobiles passing over the bridge was 1215 and 863 on Friday (weekend) and Saturday respectively. However, during the period of 3:0-5:0 P.M, the number of automobiles passing over the bridge was 780 and 975 on Friday and Saturday respectively.

From these data, it is understood that during the period of 8:0-12:0 A.M on Friday more number of automobiles were driven over the bridge so the slope of the curves (Figures 11-16) increased with a faster inclination comparing with the Saturday's data. For the period of 3:0-5:0 P.M, on Saturday, more number of automobiles was recorded, so the peak point on Saturdays' diagram is higher than Fridays' diagram.

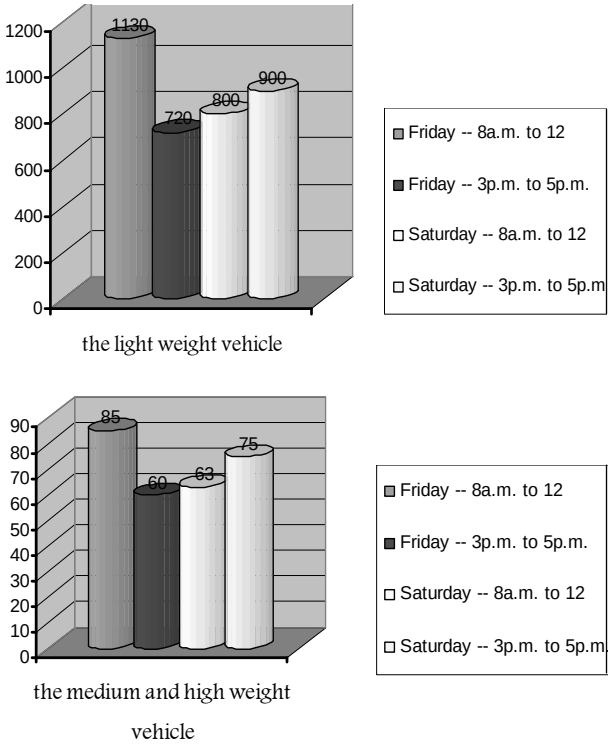

Figure 10. Diagram of number of vehicles passing over the bridge.

TABLE 2. The Number of Passing Medium and High Weight Vehicles.

Number of Passing Vehicle	Time-Period	Date
85	8-12	Friday (Novmber 25, 2005)
60	15-17	
63	8-12	Saturday (Novmber 26, 2005)
75	15-17	

TABLE 3. The Number of Passing Light Weight Vehicle.

Number of Passing Vehicle	Time-Period	Date
1130	8-12	Friday (Novmber 25, 2005)
720	15-17	
800	8-12	Saturday (Novmber 26, 2005)
900	15-17	

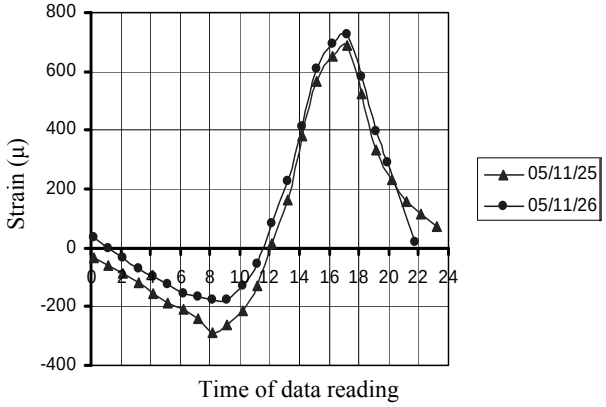

Figure 11. Field strain values for gauge No. 11 at different daily time due to daily traffic flows.

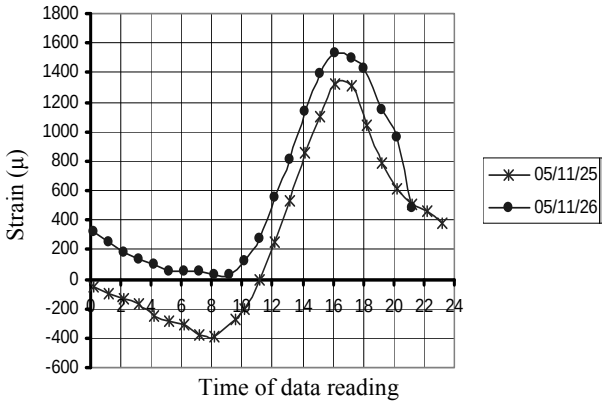

Figure 14. Field strain values for gauge No. 13-horizonal- at different daily times due to daily traffic flows.

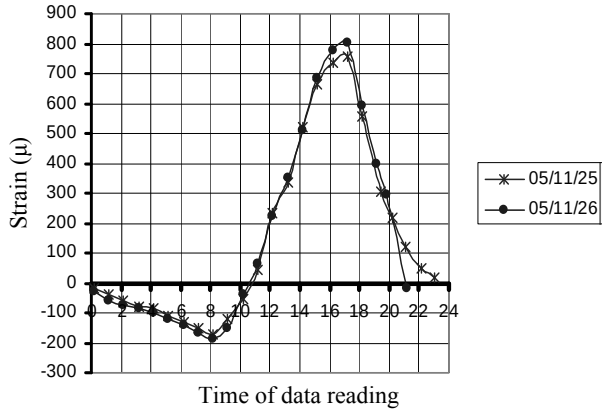

Figure 12. Field strain values for gauge No. 1 at different daily time due to daily traffic flows.

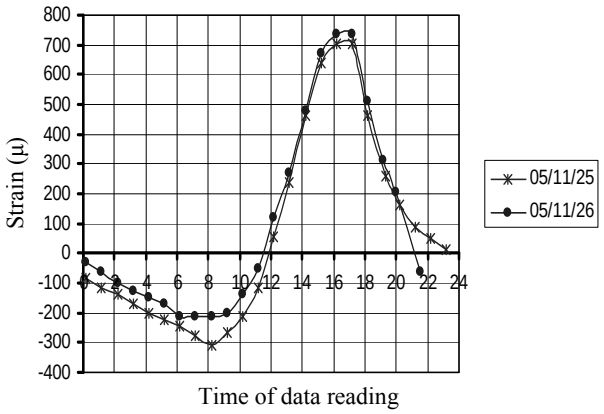

Figure 15. The amount of field strains of Gauges No. 21 at different daily times due to daily traffic flows.

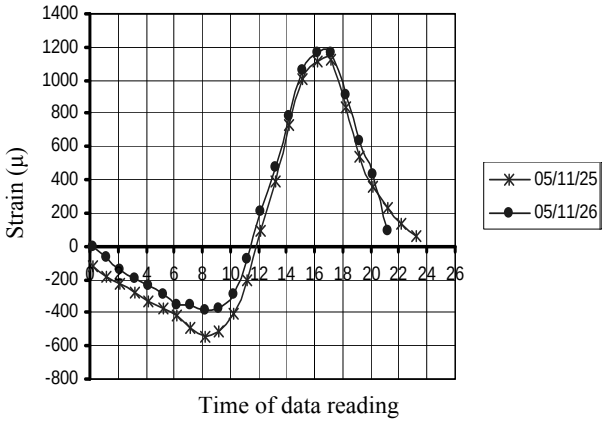

Figure 13. Field strain values for gauge No. 13-vertical-at different daily time due to daily traffic flows.

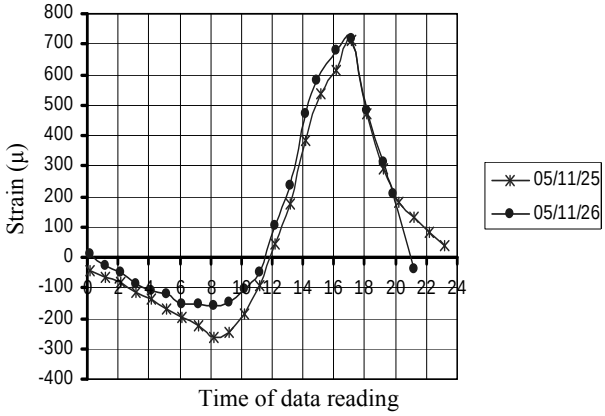

Figure 16. The amount of field strains of gauges No. 16 at different daily times due to the daily traffic flows.

4. THE THEORETICAL ANALYSES OF RETAINING WALL

Based on obtained values of strain field analyses, the theoretical analyses of RC retaining wall, RW was considered [6,11] at service conditions for the following three positions.

4.1. The Theoretical Analyses of Bottom Section of Retaining Wall Between Counterforts The bottom section properties of RW considered between counterforts are shown in Figure 17.

The geometric center and moment of inertia for uncracked equivalent section is calculated for 1m length and the values are given in Table 4.

For the values of Table 5, the extreme concrete bottom fiber is supposed as the origin axis. By considering the moment of inertia about N.A;

$$I=\sum(I_g + Ay^2) - \frac{(\sum Ay)^2}{\sum A} = 1812726.02 \text{ cm}^4 \quad (1)$$

$$\bar{y} = \frac{\sum Ay}{\sum A} = 30 \text{ cm} \quad (2)$$

It is cleared that for RC section, if the tensile stress on the extreme concrete fiber is less than the modulus of rupture, the section is uncracked. Else,

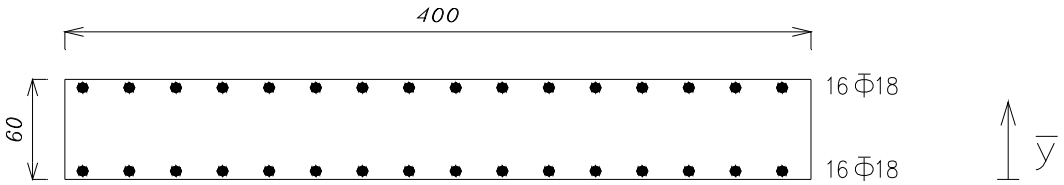

Figure 17. The bottom section between counterfourts.

TABLE 4. The Calculated Properties of Bottom Section between Counterforts.

Property	Dimension	A	y	Ay	Ay^2	I_g
Concrete Area	100 × 60	6000	30	180000	5400000	1800000
Steel Rebar	4 Φ 18	10.18	5	50.89	254.47	0.00
Steel Rebar	4 Φ 18	10.18	55	559.83	30790.75	0.00
∑		6020.36		180610.72	7231045.22	

TABLE 5. The Calculated Properties of Top Section of RW between Counterforts.

Property	Dimension	A	y	Ay	Ay^2	I_g
Concrete Area	100 × 30	3000	15	45000	675000	2500000
Steel Rebar	4 Φ 18	10.18	5	50.89	254.47	0.0
Steel Rebar	4 Φ 18	10.18	25	254.5	6362.5	0.0
∑		3020.36		45305.39	3181616.97	

the section is cracked. However, for cracked section, the elastic stresses analyses are valid while, the concrete compressive stress on the extreme fiber is less than $0.5f_c^{'}$ (Figure 18). Usually this is the situation occurred for the RC sections under service load.

$$\text{(Rupture Modulus)}\ f_r = 2\sqrt{f_c^{'}} = 31.62\ \ \text{Kg/cm}^2 \quad (3)$$

$$\sigma = \frac{M.y}{I} \Rightarrow$$
$$M_r = \frac{f_r \times I}{y} = \frac{31.62 \times 1812726.02}{30} = 19.11\ \ \text{ton} - \text{m} \quad (4)$$

The obtained negative bending moment (calculated with the related equations) in the extreme fiber is $M = 25.6$ ton.m which is more than the cracking moment (i.e., M_r = 19.11 ton.m) by Equation 4. Therefore the section is cracked and the linear analyses of cracked transformed section (the steel bars are replaced with an equivalent area of fictitious concrete (nA_s), which supposedly can resist tension and this area is referred to as transformed area) can be followed.

The cracked transformed section is formed with the compression region occurred above concrete neutral axis, and the steel area is n times the cross section area of the bars. The ratio of the steel modulus to the concrete modulus is called the modular ratio n $(n = E_S/E_C = 8.8)$. This is shown in Figure 19.

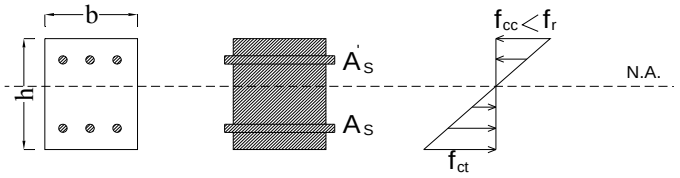

The uncracked reinforcement concrete section

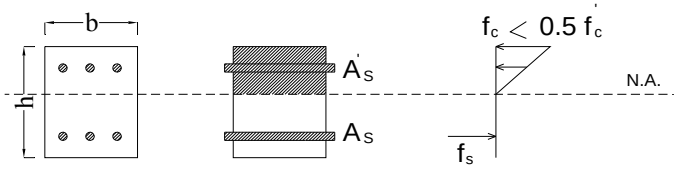

The cracked reinforcement concrete section

Figure 18. The limitation of cracked and uncracked.

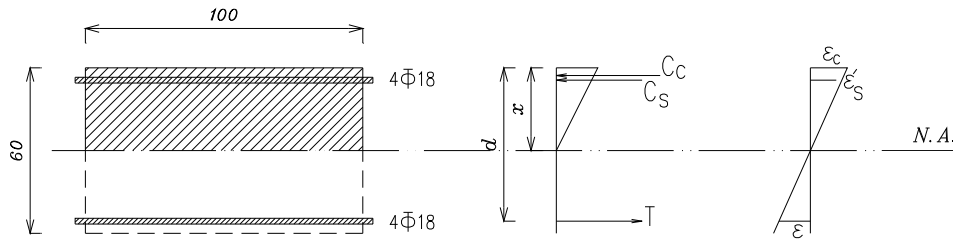

Reinforcement Concrete Section Stress Diagram Strain Diagram

Figure 19. The cracked transformed section of the bottom.

The moment of the compression area of the RW cross section about the neutral axis (N.A) must equal the moment of the tensile area about the neutral axis. The resulting quadratic equation can be solved by completing the squares.

After the neutral axis is located, the moment of inertia of the transformed section is calculated, and the stresses in the concrete and the steel are computed with the flexural formula.

$$\frac{bx^2}{2}+nA_s^{'}(x-5)=nA_s(d-x) \Rightarrow x = 8.73 \text{ cm} \qquad (5)$$

The tension and compression stress in the extreme fiber are calculated as:

$$\sigma_{cc}=\sigma_{ct}=42.36 \quad Kg/cm^2$$

and

$$f_{c,max}=\frac{f_c^{'}}{2}=125 \quad Kg/cm^2 \qquad (6)$$

The compressive stress in the extreme concrete fiber is less than the limited elastic value and therefore, the concrete has a linear action. The stresses and strains in each fiber can be calculated as followed:

The moment of forces in the stress diagram (shown in Figure 19) related to the center of gravity of concrete compression force (C_C) is calculated:

$$\begin{aligned} &C_S\times(5-8.73/3)-T\times(55-8.73/3)=M \\ &\Rightarrow 2.09C_S-52.09T=M \end{aligned} \qquad (7)$$

$$C_S=A_S^{'}.E\varepsilon_S^{'} \quad ; \quad T=A_S.E\varepsilon_S \qquad (8)$$

Considering the strain diagram shown in Figure 19:

$$\frac{\varepsilon_S^{'}}{x-5}=\frac{\varepsilon_S}{d-x} \Rightarrow \varepsilon_S=12.4\varepsilon_S^{'} \qquad (9)$$

Substituting Equations 8 and 9 into Equation 7:

$$\therefore \varepsilon_S^{'}=186\times10^{-6} \quad ; \quad \varepsilon_S=2307\times10^{-6} \qquad (10)$$

4.2. The Theoretical Analyses of Top Section of Retaining Wall Between Counterforts

The top section properties of RW considered between counterforts are shown in Figure 20. As before, for uncracked transformed section, the center of geometer and moment of inertia are calculated as; for these values, the extreme bottom fiber is supposed as the origin axis. Considering the moment of inertia about N.A;

$$I=\sum(I_g+Ay^2)-\frac{(\sum Ay)^2}{\sum A}=2502036.27 \text{ cm}^4 \qquad (11)$$

$$\bar{y}=\frac{\sum Ay}{\sum A}=15 \text{ cm} \qquad (12)$$

For free edge of the slab, one-third of the calculated negative moment was assumed. So, the moment in the extreme fiber is M = 4 ton.m. Based on Figure 18, the moment for extreme fiber is less than the cracking moment (M_r), and therefore the analyses of the section are assumed as uncracked section. For uncracked section, the stress in tensile bars can be calculated as:

$$\begin{aligned} &f_S=n\frac{M.y}{I}=8.8\times\frac{11030/3\times100\times10}{2502036.27}= \\ &12.93 \text{ kg/cm}^2 \Rightarrow \varepsilon_S=6.16\times10^{-6} \end{aligned} \qquad (13)$$

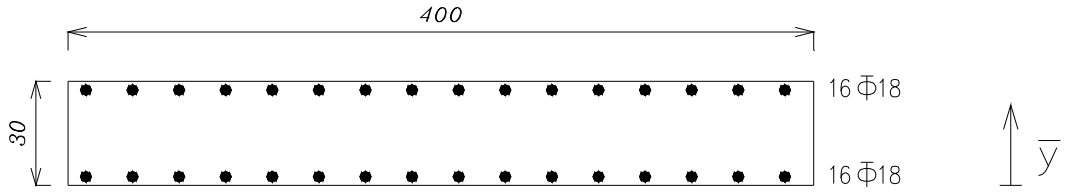

Figure 20. The top section of RW between counterforts.

4.3. The Theoretical Analyses of The Retaining Wall at the Position of Counterforts The counterforts are like the prismatic cantilevers that are concreting with the heel slab. Therefore, such position acts as a T-beam, on which the retaining wall slab is treated like a web and the counterfort as a flange of T-beam. The maximum value of bending moment is occurred due to the soil pressure at the bottom of the wall. This studied section is shown in Figure 21. According to the ACI code, the effective width of the T-beam is:

$$b = \min.\begin{cases} \frac{L}{4} = \frac{700}{4} = 175 \text{ cm} \\ 16\,h_f + b_w = 1005 \text{ cm} \\ 445 \text{ cm} \end{cases} \Rightarrow b = 175 \text{ cm} \quad (14)$$

The value of soil horizontal pressure at bottom of the wall is $(P_h = 5231 Kg/m^2)$. The center to center distance of two adjacent counterforts is known, and therefore the bending moment at the bottom section of the wall is:

$$P = 5231 \times 4 = 20924 \text{ kg/m} \rightarrow$$
$$M = 20924 \times 7/2 \times 7/3 = 170879.33 \text{ kg.m} \quad (15)$$

$$\bar{y} = \frac{\sum Ay}{\sum A} = 110.53 \rangle t_f = 60 \text{cm} \Rightarrow \text{T - beam} \quad (16)$$

$$I = \sum (I_g + Ay^2) - \frac{(\sum Ay)^2}{\sum A} = 193559302 \text{ cm}^4 \quad (17)$$

Referring to Equation 15, the moment for the analyzed section is M = 170.8 ton-m. Similar to previous parts, as the calculated moment is less than the cracking moment, therefore the section is uncracked as it was supposed. The steel rebar strains can be calculated as followed:

a-For steel rebar at bottom section of the counterfort:

$$f_S = n\frac{M.y}{I} = 8.8 \times \frac{170879.33 \times 100 \times 189.47}{193559302} =$$
$$147.2 \text{ kg/cm}^2 \Rightarrow \varepsilon_S = 70.1 \times 10^{-6} \quad (18)$$

b-For steel rebar at bottom of the retaining wall

$$f_S = n\frac{M.y}{I} = 8.8 \times \frac{170879.33 \times 100 \times 55.53}{193559302} =$$
$$43.14 \text{ kg/cm}^2 \Rightarrow \varepsilon_S = 20.5 \times 10^{-6} \quad (19)$$

$$f_S = n\frac{M.y}{I} = 8.8 \times \frac{170879.33 \times 100 \times 105.53}{193559302} =$$
$$81.98 \text{ kg/cm}^2 \Rightarrow \varepsilon_S = 39.04 \times 10^{-6} \quad (20)$$

The equations for uncracked transformed section (Figure 22) are used and the calculated values are given in Table 6.

4.4. Analyzing of Retaining Wall Considering Finite Element "ANSYS" Method The model divided to elements in finite element method and so the model can be analyzed by using these fine elements. Each element has some nodes that all the input and output data related to the nodes. During analyzing of a model with the finite element model, as many as 20,000 equations-should be solved at the same time. The number of equations is related to the number of elements and their nodes. The structure of retaining wall is modeled using ANSYS. This software was designed by an American company Swanson in 1971. The software is capable to analyze the nonlinear and failure mode of the member.

The modeling can be done easier while using the symmetrical conditions [12,13]. The concrete was modeled by solid 65 elements. Such an element has eight nodes with three degrees of freedom at each node-translation in the nodal x, y, and z directions. The assumed element is capable of carrying plastic deformation, cracking in three orthogonal directions, and crushing. A link8 element was used to model the steel reinforcement. Such element is a 3D spar element and it has two nodes with three degrees of freedom-translations in the nodal x, y, and z directions [7-10].

The solid 65 element requires linear isotropic and multilinear isotropic material properties to properly model concrete. The multilinear isotropic material uses the Von Mises failure criterion to define failure of the concrete. The compressive uniaxial stress-strain relationship for the concrete model was obtained using the equations to compute the multilinear isotropic concrete stress-strain curve [12].

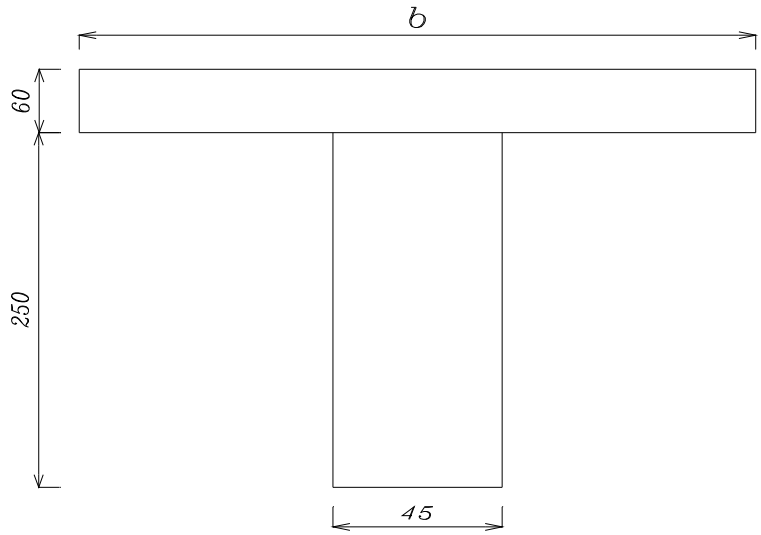

Figure 21. The section studied at the position of counterforts.

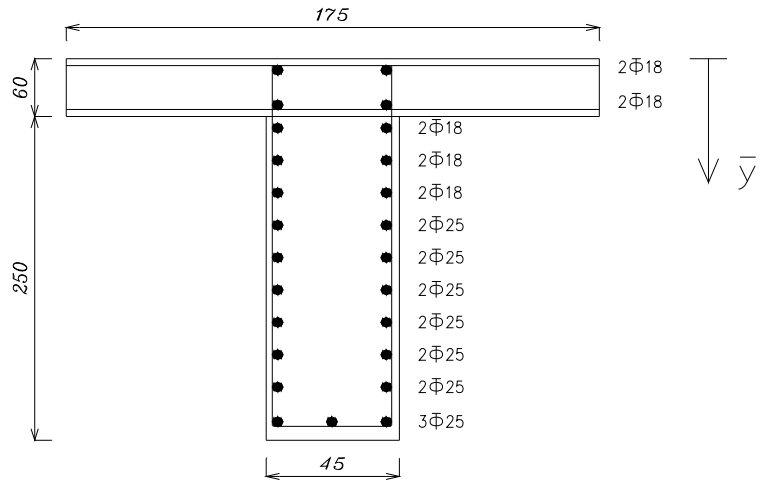

Figure 22. The bars in the section studied at position of counterforts.

4.5. Modeling, Loading and Boundary Conditions The symmetry conditions were used to model the structure. This structure has 8.3 meter height and 4.65 meter length between two walls (Figure 23). To ensure that the model acts as close to the real structure as possible, boundary conditions needed to be applied at points of symmetry, and where the supports and loading exists.

To model the symmetry, nodes on this plane must be constrained in the perpendicular directions, so they have degree of freedom constraint $U_x = 0$ and $U_z = 0$. The next step is loading, and based on the real structure, the truck loads are used.

4.6. The ANSYS Analyzing The options for nonlinear analyzing and controlling the output data are summarized in Tables 7-9. The options are the same as the program assumptions. By using these options, the structure is modeled with 214500 element of solid65 and 302207 element of link8. The ANSYS modeling of the structure is shown in Figure 24.

TABLE 6. The Calculated Properties of the Section at the Position of Counterfort.

Property	Dimension	A	y	Ay	Ay^2	I_g
Concrete Area	175 × 60	10500	30	315000	9450000	3150000
Concrete Area	250 × 45	11250	185	2081250	385031250	58593750
Steel Rebar	3 Φ 25	14.73	300	4417.86	1325359.4	0.0
Steel Rebar	2 Φ 25	9.82	275	2699.81	742446.7	0.0
Steel Rebar	2 Φ 25	9.82	250	2454.37	613592.32	0.0
Steel Rebar	2 Φ 25	9.82	225	2208.93	497009.78	0.0
Steel Rebar	2 Φ 25	9.82	200	1963.5	392699.08	0.0
Steel Rebar	2 Φ 25	9.82	175	1718.06	300660.23	0.0
Steel Rebar	2 Φ 25	9.82	150	1472.62	220893.23	0.0
Steel Rebar	2 Φ 18	5.09	125	636.17	79521.56	0.0
Steel Rebar	2 Φ 18	5.09	100	508.94	50893.8	0.0
Steel Rebar	2 Φ 18	5.09	75	381.7	28627.76	0.0
Steel Rebar	2 Φ 18	5.09	50	254.47	12723.45	0.0
Steel Rebar	2 Φ 18	5.09	5	25.45	127.23	0.0
∑		21849.1		2414991.88	460489554.5	

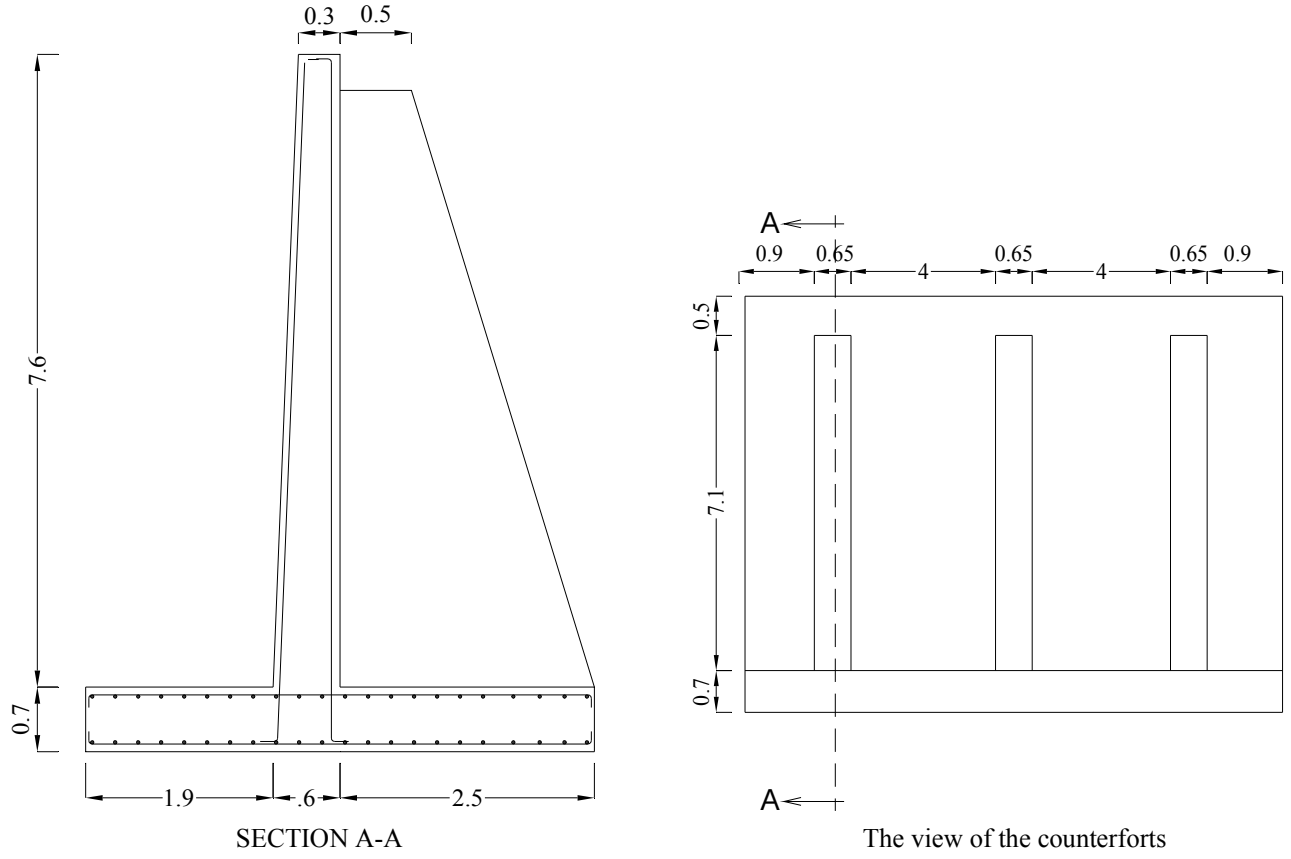

Figure 23. The conditions of the structure and its counterforts.

TABLE 7. The Options of Controlling Nonlinear Analyzing.

Program Behavior Upon Nonconvergence	Terminate but do not exit
Nodal DOF Sol'n	0
Cumulative Iter	0
Eplased Time	0
CPU Time	0

TABLE 8. The Options of Nonlinear Analyzing.

Analyzis Option	Small Displacement
Calculate Prestress Effects	No
Automatic Time Stepping	On
Number of Substeps	1
Max no. of Substeps	2
Min no. of Substeps	1
Write Items to Results File	All Solution Items
Frequency	Write Every Substep

TABLE 9. The Options of Controlling Output Data.

Equation Solvers	Sparse Direct
Number of Restart Files	1
Frequency	Write Every Substep

5. COMPARISON OF RESULTS

In this investigation, the analysis of the bridge structure was performed under traffic loads, by three different methods to find out the strains on the reinforcement steel; (1) the strain field were analyzed by the data recorded on the electrical strain gauges, (2) the theoretical strain analyzing, and (3) the strains obtained by the ANSYS modeling and the results are compared (Table 10).

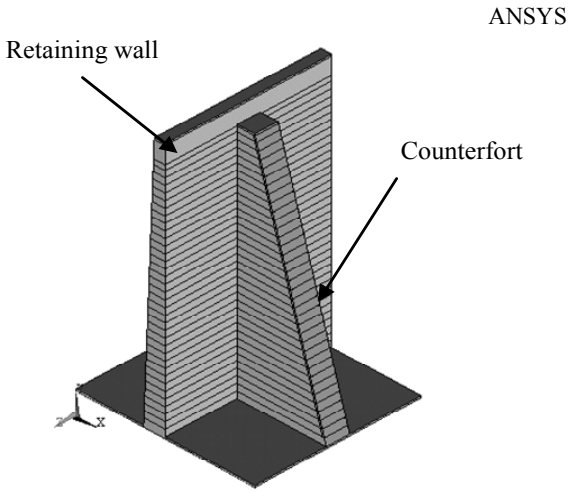

Figure 24. The modeling for retaining wall in ANSYS software.

TABLE 10. The Results of Each case of Bridge Analyzing.

Strain Gauge Position	Strain Due to Field Analyzing	Strain Due to Theoretical Analyzing	Strain due to ANSYS Modeling
S.G.1	65×10^{-6}	39.04×10^{-6}	50×10^{-6}
S.G.11	90×10^{-6}	20.5×10^{-6}	76×10^{-6}
S.G.13 (h)	200×10^{-6}	20.5×10^{-6}	184×10^{-6}
S.G.13 (v)	170×10^{-6}	20.5×10^{-6}	139×10^{-6}
S.G.16	150×10^{-6}	70.1×10^{-6}	131×10^{-6}
S.G.21	100×10^{-6}	6.16×10^{-6}	85×10^{-6}

6. CONCLUSIONS

To study the field analysis of RC bridge for the service life history, the structural health monitoring, SHM technique was adopted. The bridge was loaded with different loading arrangements to record the steel strains. The theoretical analysis and the Finite Element modeling were also performed. The results of three methods are compared and the following conclusions were drawn;

- The results obtained by ANSYS modeling of the structure are close to the field analysis results. However, the small variations of the results for two methods are acceptable and it is mainly due to the assumed meshing system (i.e., the number of elements considered in the solid65 and link8) in F.E program.
- The differences of theoretical and field analyzing method are about 30-40 %. This could be due to the estimated values of E_c, f_r,... recommended by different Codes of practice in elastic behavior of the RC structures and also the rate of strain changes as creep, temperature, … are occurred in real structures.
- Based on the values of field steel strains recorded, it is obvious that the traffic load of automobiles passing over the bridge have no excessive effects on the behavior of retaining wall. In other words, it seems the retaining wall is designed conservatively.
- The results obtained by three methods indicated that, the bridge under the traffic loads are threaded linearly, in other words, it could be loaded more than what it was designed for. However, the more exact analysis of the bridge is possible by installing the different type of sensors such as stability pressure gauges on different parts of the bridge.

7. REFERENCES

1. Wahbeh, M. and Masri, S. F., "Real-Time Structural Monitoring of Large Scale Bridge Structures", Dep. of Civil Engineering, University of Southern California, California, U.S.A., (2005).
2. Yang, X., "Cement-Based Piezoelectric Sensing System For Structural Healthy Monitoring", School of Civil Engineering, Tianjin University, China, (2005).
3. Huntington, W. C., "Earth Pressures and Retaining Walls", John Wiley and Sons, Inc., New York, U.S.A., (1957).
4. http://www.ramboll.com (Ramboll Group A/S, Head OfficeTeknikerbyen1, 2nd Floor DK-2830 Virum Denmark), E-mail: info@ramboll.com.
5. Azadpour, F., "The Field Analyses of the Pajouhesh Square by SHM," M.Sc. Thesis, Supervised by, Maghsoudi, Civil Eng. Dept., Kerman University, Kerman, Iran, (2005).
6. Ramezanianpour, A. A. and Maghsoudi, A. A., "Design of Reinforced Concrete Structures", Science and Culture Publication, Tehran, Iran, (1997).
7. Fanning, P., "Nonlinear Models of Reinforced and Post-tensioned Concrete Beams", ***Electronic Journal of Structural Engineering***, University College Dublin, Earlsfort Terrace, Dublin 2, Ireland, (September 12, 2001), 111-119.
8. Kachlakev, D. I., Miller, T., Yim, S., Chansawat, K. and Potisuk, T., "Finite Element Modeling of Reinforced Concrete Structures Strengthened With FPR Laminates", California Polytechnic State University, San Luis Obispo, CA and Oregon State University, Corvallis, OR for Oregon Department of Transportation, California, U.S.A., (May 2001).
9. Tavarez, F. A., "Simulation of Behavior of Composite Grid Reinforced Concrete Beams Using Explicit Finite Element Methods", Master's Thesis, University of Wisconsin-Madison, Madison, Wisconsin, U.S.A., (2001).
10. Gabriel, J. and Desalvo, R., "ANSYS Engineering Analysis System Examole Manual", Swanson Analysis Systems Publication, U.S.A., (1987).
11. MacGregor, J. R, "Reinforced Concrete Mechanics and Design", Prentice Hall, Inc., Englewood Cliffs, N.J., U.S.A., (1954).
12. Shaabanali, M. R., "The Analysis of F.M. by the help of ANSYS", Sepehr Publication, Tehran, Iran, (Spring 2001).
13. Jahed-Motlagh, H. R., Noban, M. R. and Eshraghi, M. A., "ANSYS", Science and Industrial Iran University Publications, Tehran, Iran, (2003).